

Dynamic submicron particulate behavior in turbulent media

STL-008-20, Year 2 of 3

Clare Kimblin (PI), Ian McKenna, Paul Taylor, Roy Abbott, Rick Allison,
Matt Staska, Jonathon Rivera (STL), Mary O'Neill (Keystone), Jason Sears, Jens von der Linden, Chris Kueny (LLNL),
Joshua Mendez-Harper, Professor Josef Dufek (Univ. of Oregon)

This work was done by Mission Support and Test Services, LLC, under Contract No. DE-NA0003624 with the U.S. Department of Energy and supported by the Site-Directed Research and Development Program. DOE/NV/03624--1207.



Support identification, prediction and detection of HE test signatures

- Provide system and controlled experiments to address gaps that large-scale field tests (with myriad variables) cannot.
 - *Supports* predictive models of prompt **RF emission** and **particulate evolution** by providing means to answer questions:
 - How do carbon-based particulates contribute to RF/optical signatures?
 - Does additional shock impact particulate evolution?
 - *Measure RF & electrostatic conditions associated with C detonation product (CDP) materials in shocked gas*
 - *System supports correlation of late-time recovered particulates to test conditions*
 - Leverage diagnostics and algorithms from small-scale tests for large-scale tests
 - mm-wave antennas and other diagnostics are 'fielded' at STL shock tube first
 - RF and optical analysis tools developed for small-scale tests are now used for large-scale test data analysis as well

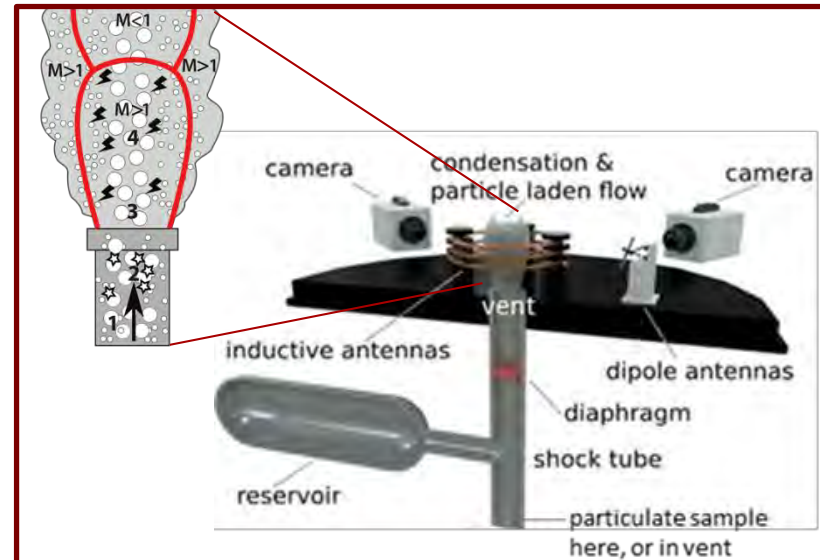
Innovation: Shock Tube Overpressure Apparatus and Diagnostics

STOA permits isolation of real-time RF emission component, with known materials, and provides improved understanding of physical phenomena that are the basis for observed field experiment signatures.

Table 1. Species Composition at the CJ State for Various Explosives*

Species	TNT mol/kg	Comp B mol/kg	LX-10 mol/kg	NM mol/kg	AP-NM mol/kg	TRITONAL mol/kg	PETN mol/kg
H2O	8.04	8.061	6.695		16.7	4.85	
CO2	7.491	7.045	6.813		6.702	1.146	
N2	6.286	10.29	12.63		5.301	4.773	
OH-	1.798	3.645	5.144		1.199	0.8374	
H+	1.798	3.645	6.511		4.076	0.8374	
CO	1.576	0.9256	1.906		0.0152	2.05	
NH3	0.632	0.7089	0.3924		0.000394	1.018	
CH4	6.69E-02	2.24E-02	1.11E-03		0	0.461	
H2	2.10E-02	6.92E-03	3.26E-04		0.000466	0.164	
C2H4	1.37E-02	3.39E-03	—		0	0.176	
C graphite	21.6	0	0	1.593	0	0.231	0
C diamond	0	12.7	7.162	0	0	0	0
C liquid	0	0	0	0	20.2	2.385	
Al2O3	0	0	0	0	3.71	0	

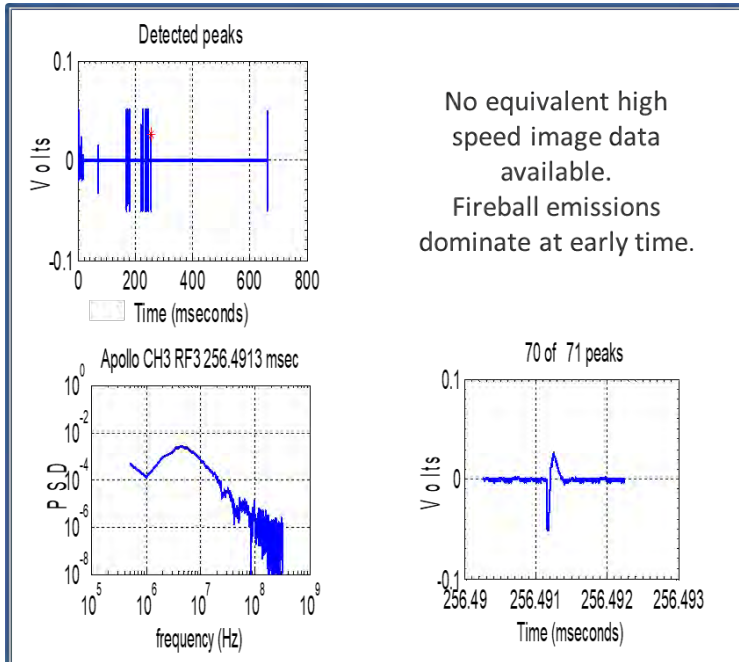
A. L. Kuhl, "Carbon Particles Produced by Detonation Waves,"
LLNL-CONF-703005, Sept. 2016



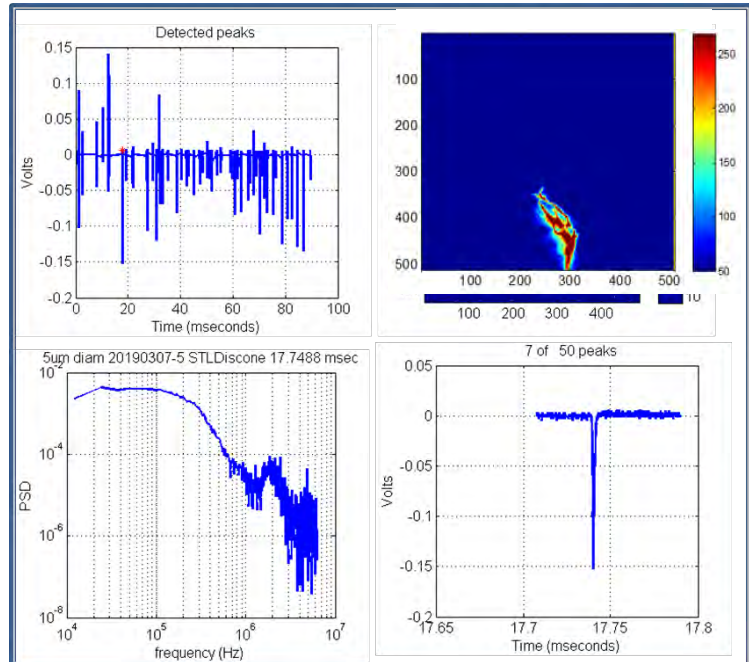
STOA components with close-up of standing shock

Large-scale RF emissions can be mimicked with small-scale shock tube

Field Test Results



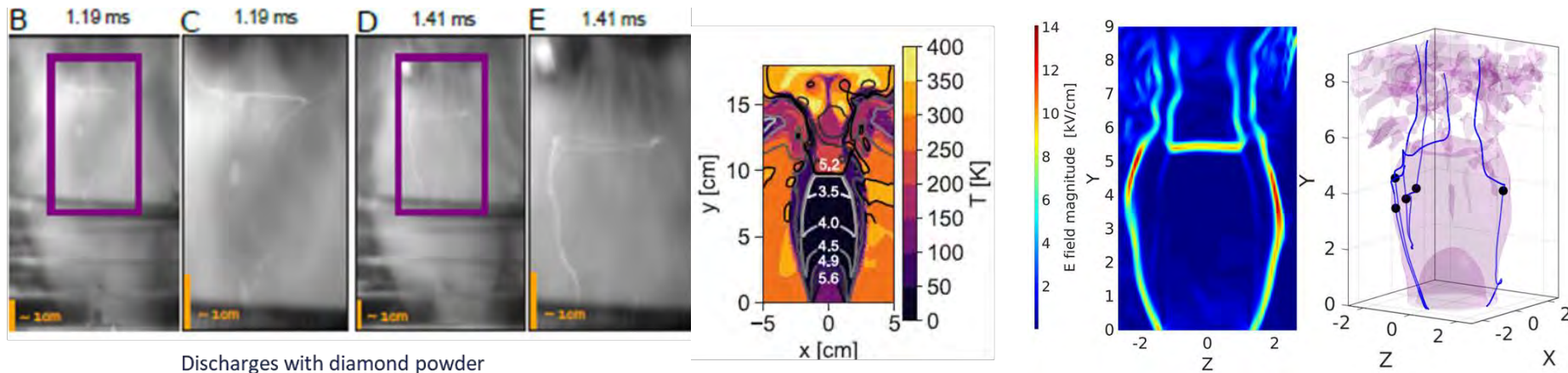
Shock Tube Results



- Significant similarities in RF output, despite field data signal amplitude being higher
- Field data were collected with a faster O-scope: higher frequency PSD

Observable Shock Structure and Discharges with Diamond

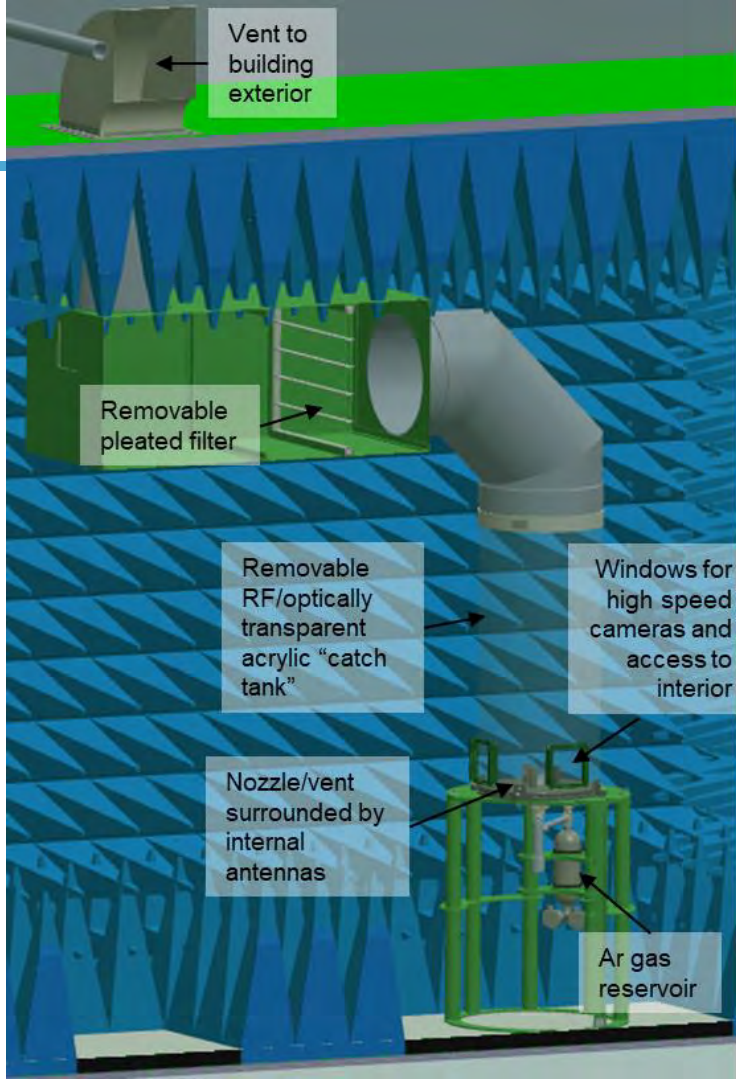
- Infinite reservoir and reduced particle quantities permit focus on observable shock interface
- STOA reproduces essential hydrodynamic and electrostatic aspects of HE test events in well-characterized environment



Manuscript “Standing shock prevents propagation of sparks in supersonic explosive flows” demonstrating consistency between experiment and LLNL models, accepted by Communications Earth & Environment

Technical Approach

- ▶ New anechoic chamber and improved shock tube
 - Better particle exhaust
 - Removable catch tank for cleaning or replacement
 - Optional nozzle-based sample delivery
 - For reduced particle-to-wall charging and near-vent particle entrainment
- ▶ Diagnostic improvements
 - 'Isolated' DC pressure transducer (P_{trans}) at nozzle
 - Higher frequency RF measurements (35 GHz w/ block down-conversion method)
 - Faraday cups to measure particle charge
 - Rogowski coil to determine discharge polarity
- ▶ Fluidized bed studies (U of OR)
- ▶ Analytical tool improvements

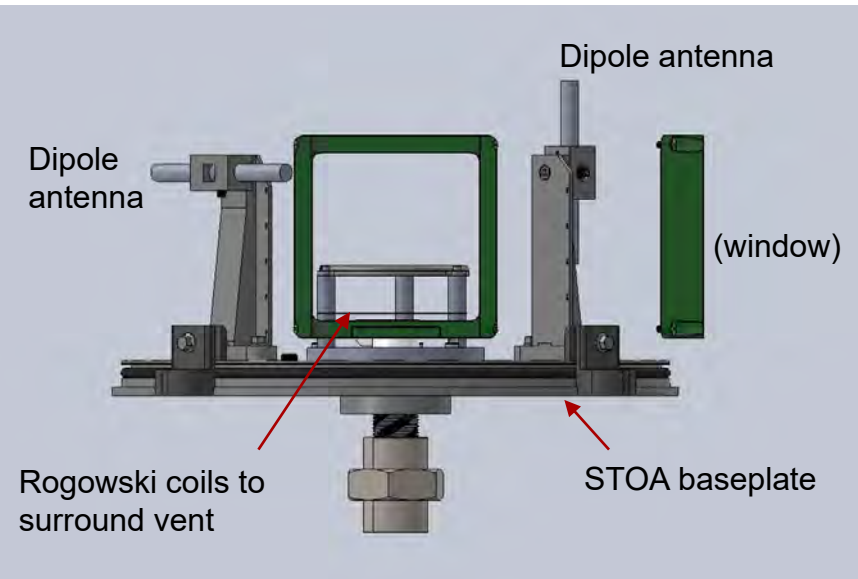


RF and Anechoic Chamber SME: Paul Taylor;
STOA and exhaust design by Matt Staska and Roy Abbott.

Internal and external RF antennas

7

Internal antennas, mounts, and feedthroughs:



Faraday cup and conductivity probe feedthroughs to be added

Antennas will span DC to 40 GHz:

Antenna	freq. range	location
2 Rogowski coils	DC to 40 MHz	internal
2 cross dipoles	.7 to 2.5 GHz	internal
E-field rod antennas	30 Hz to 50 MHz	external
Monopole	100 Hz to 60 MHz	external
Biconical 1 (qty. 4)	20 MHz to 330 MHz	external
Biconical 2	30 MHz to 1 GHz	external
→ Active Discone	100 Hz to 1 GHz	external
→ Double ridge single pol	1 to 12 GHz	external
→ Quad ridge Horn	2 to 18 GHz	external
Lensed Horn	32 to 40 GHz	external

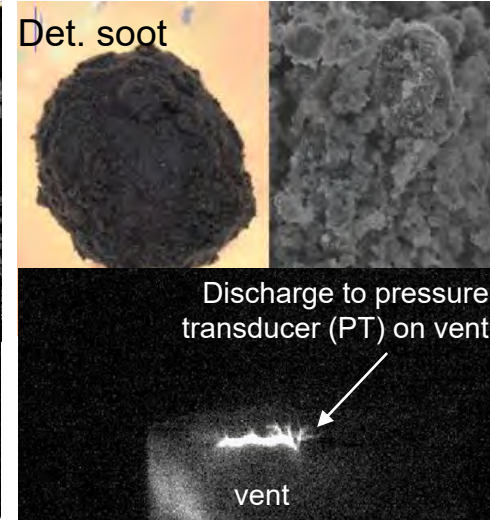
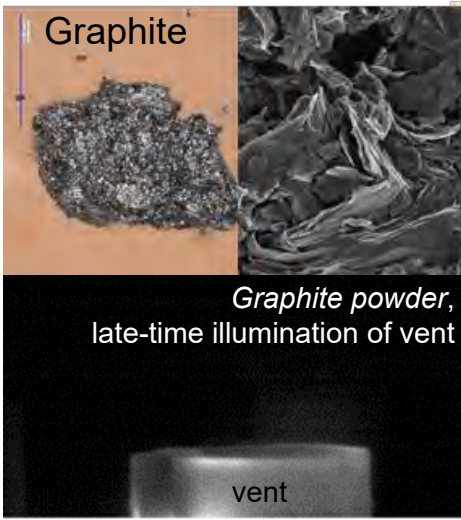
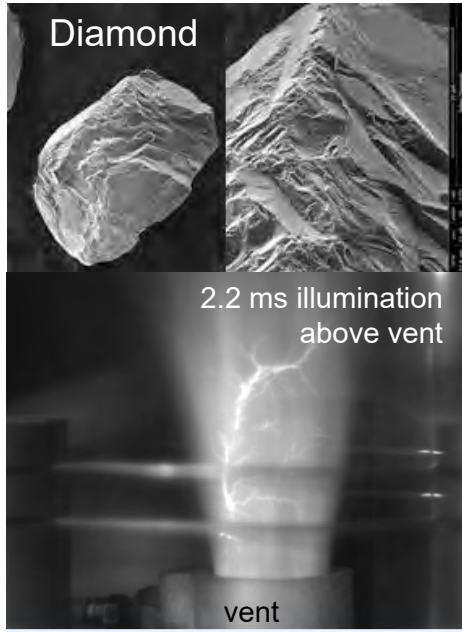
Shorter discharges associated with higher turbulence, and higher frequency RF emissions

- If discharge with length 'l' treated as monopole antenna, max RF radiation expected at $f = c/4l$
 - ≤ 1 mm discharges \Rightarrow 10's of GHz range RF

Previous measurements limited to 312 and 625 MHz by antenna selection and scope sampling rates

Down-conversion will be used to capture >10 GHz

Rapid decompression experiments: Carbon allotropes



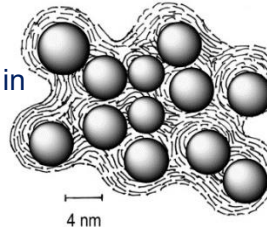
With sp^2 C, discharges not observed *during* sample ejection

Discharges *within* vent at later times

Detonation soot compositions vary:

- CompB detonation soot (~50% diamond)
- TNT soots are graphitic

Model of core nanodiamond (ND) in amorphous soot
Kruger *et al.*, 2005



Fluidized bed and vibrating ramp measurements – U of OR

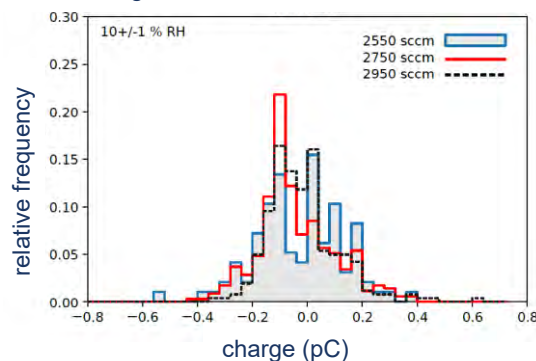
Fluidized bed: Diamond and graphite particle-to-particle charging (A, B)

- Faraday cup indicates conservation of charge (A, B)
 - With diamond having broader charge distribution relative to graphite.

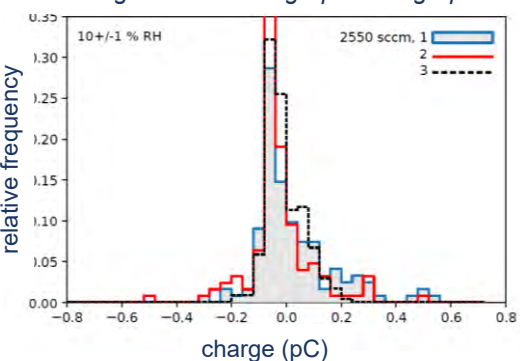
Vibrating ramp: Particle-to-wall and particle-to-particle charging (C, D)

- Vibrating ramp (D) required to break up particles highly prone to aggregation.
- Diamond, GR, and DS (est. $\phi \sim 4.8$) charge negatively against stainless steel ($\phi \sim 4.4$) and Al ($\phi \sim 4.1-4.4$) (C)
- *Diamond has broadest charge distribution*
- Effect of PMMA?

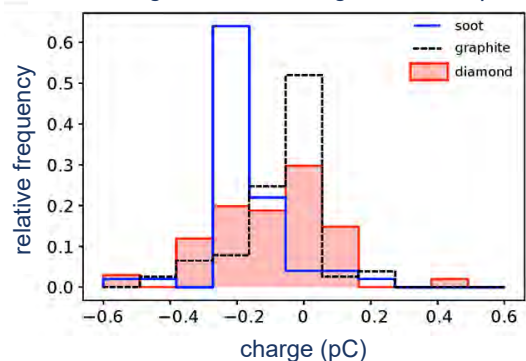
A. Charge distribution: diamond-to-diamond



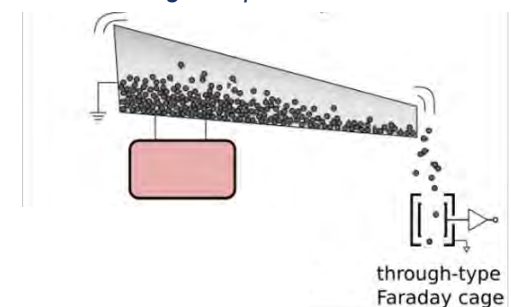
B. Charge distribution: graphite-to-graphite



C. Charge distribution: against Al ramp



D. Vibrating Ramp

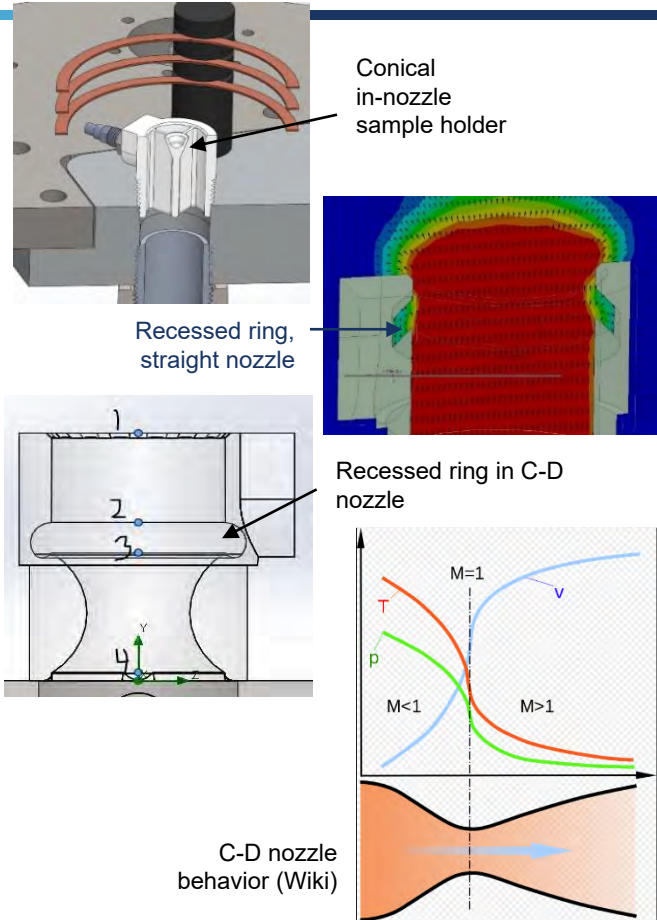


Broader charge distribution with diamond relative to Graphite and Comp B soot.

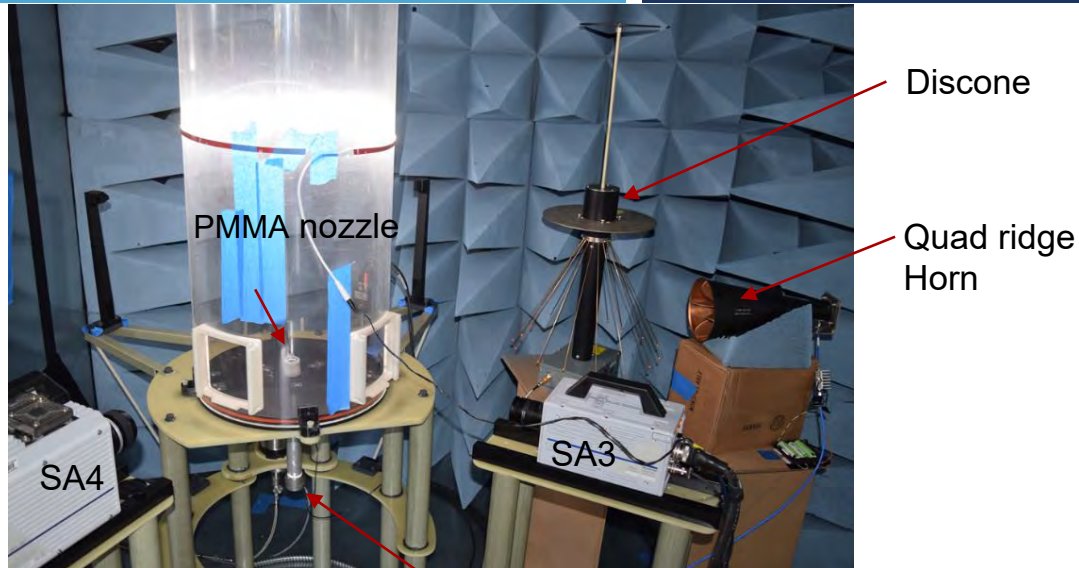
Introduction of small sample quantities from nozzle

In-nozzle sample holder

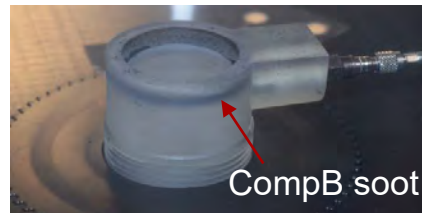
- For reduction in particle-to-wall charging relative to particle-to-particle charging
 - Important for small (<100 mg) sample quantities
- For controlled release of small sample quantities into standing shock wave
 - Restricted quantity may be due to limited sample availability, or desire to create low particulate concentration conditions for modeling
 - May allow for sequential ejection of different types of particles (e.g., micro-diamond into soot)
- Design considerations
 - Sufficient volume for sample (~ 0.25 mL)
 - Sufficient particle evacuation rate for particle-to-particle charging
 - Does not alter flow so as to prevent Mach Disk from forming above nozzle
- FlowSim to guide 3D printing of optimal PMMA nozzle(s)
 - Straight and Convergent-Divergent (C-D) nozzle



Preliminary Experiments

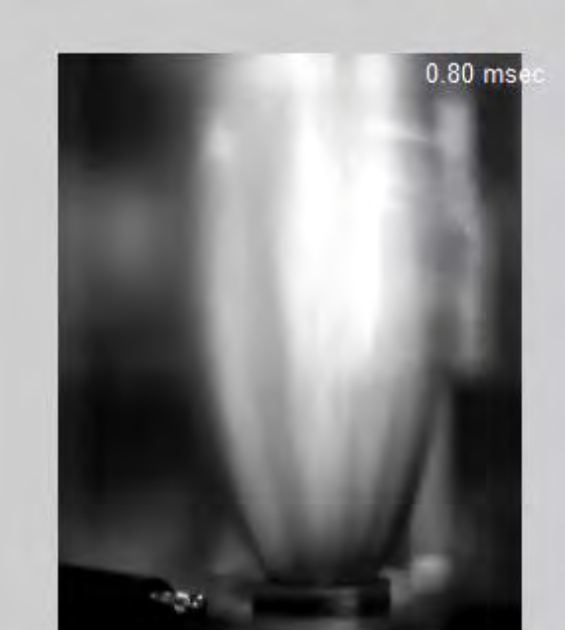


Particulates can be loaded in Al shock tube, or PMMA nozzles (below)



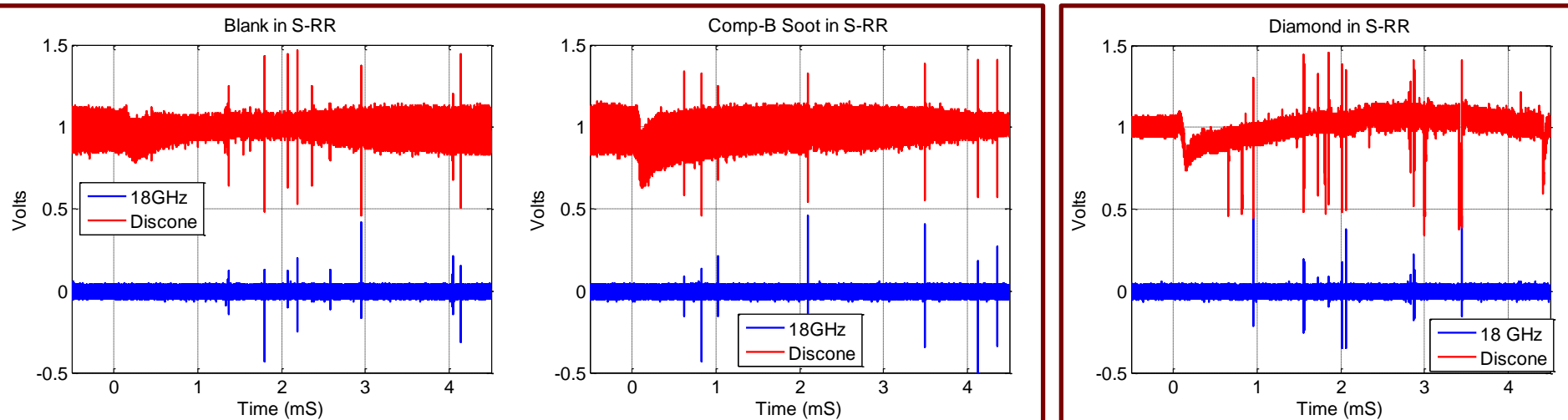
Straight RR Nozzle: Blank (left – S07), CompB soot (middle – S08), Diamond (right – S09)

12



Less clumpy, Comp B soot appears to be released more rapidly than diamond powder.

Straight RR Nozzle Releases: Blank (LHS) vs. ice-captured CompB soot (middle) vs. diamond (RHS)

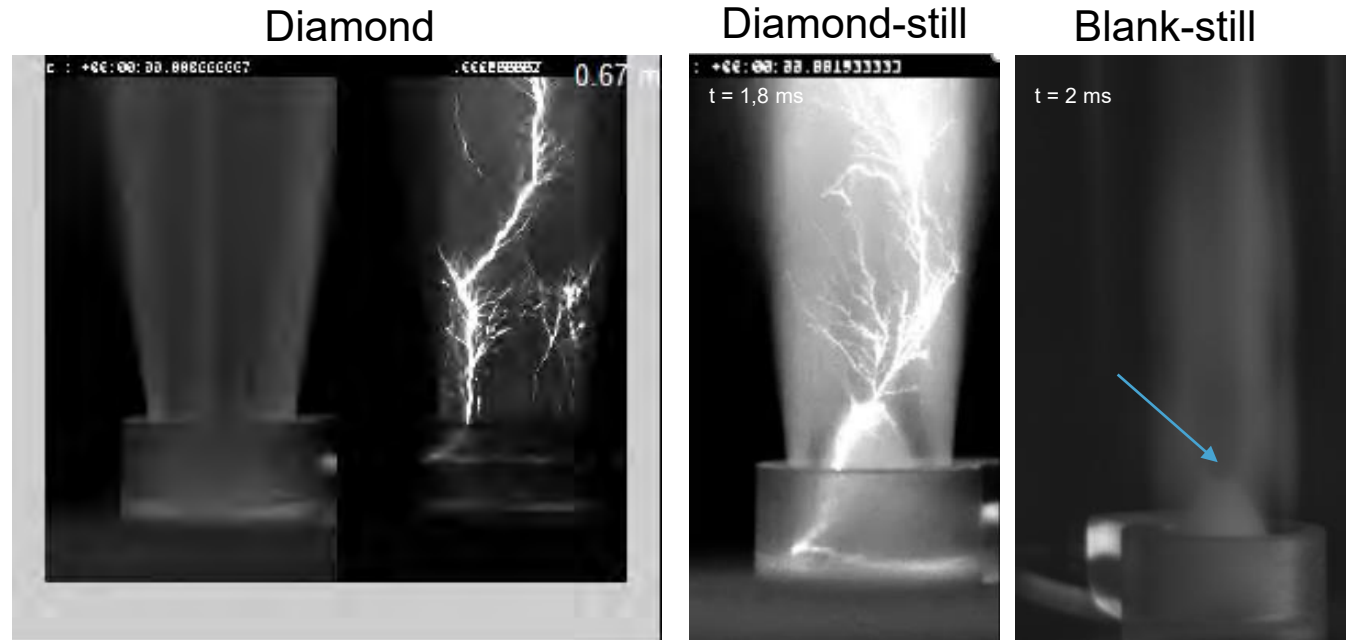
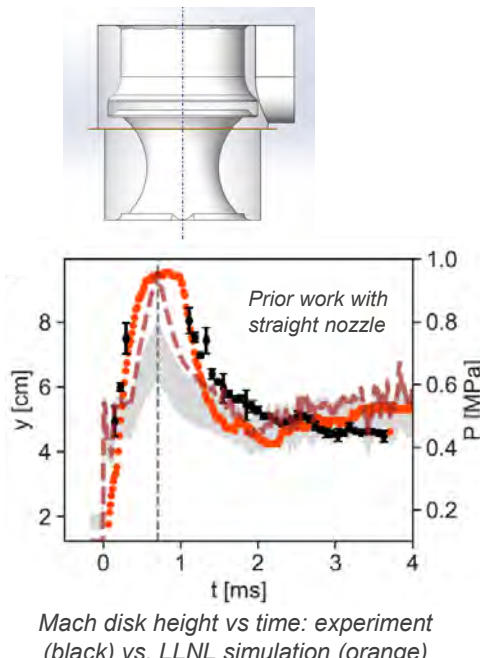


Initial comparison of number and magnitude of RF emission pulses from Comp B soot (in nozzle) vs. Blank suggests soot is not producing significant RF.

- Lower pressure, insufficient contact charging?

More plentiful RF pulses from diamond (in nozzle) suggests sufficient contact charging.

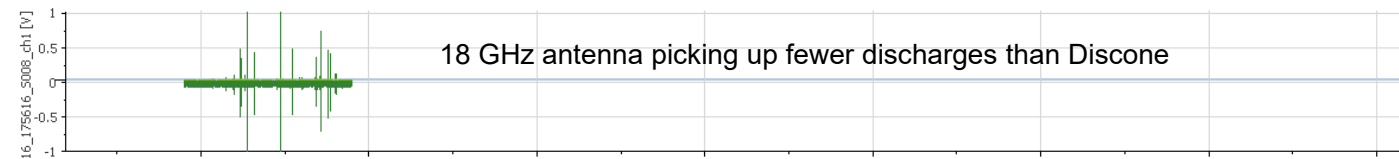
CD-RR Nozzle Releases: Diamond (left – S09), Blank (right – S07)



Sufficient turbulent mixing for discharges with diamond.
Discharges constrained by Mach Disc?

CD-RR Nozzle Releases: Diamond S08 (2021.09.16)

Quadrige
1 to 6.25 GHz



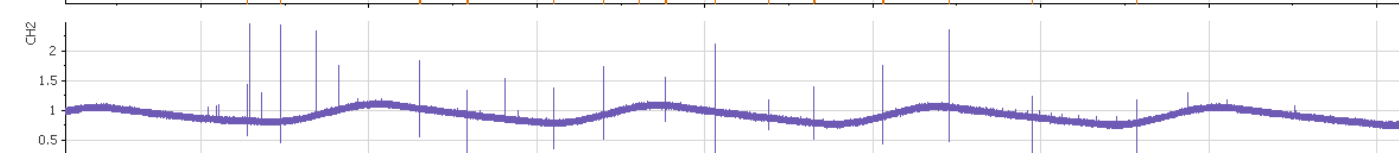
Discone
to 1 GHz



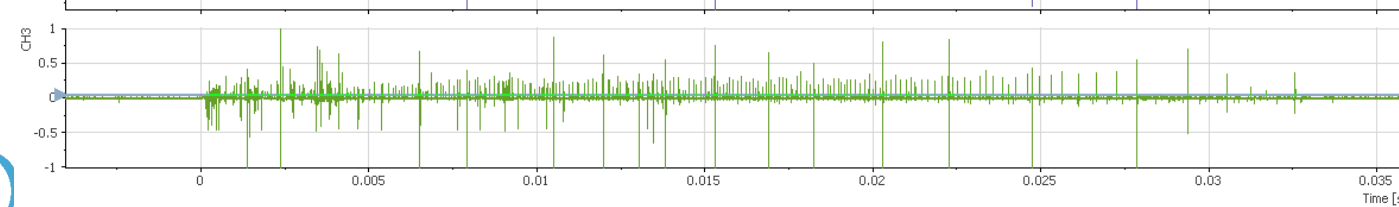
PTn (picking up
discharges)



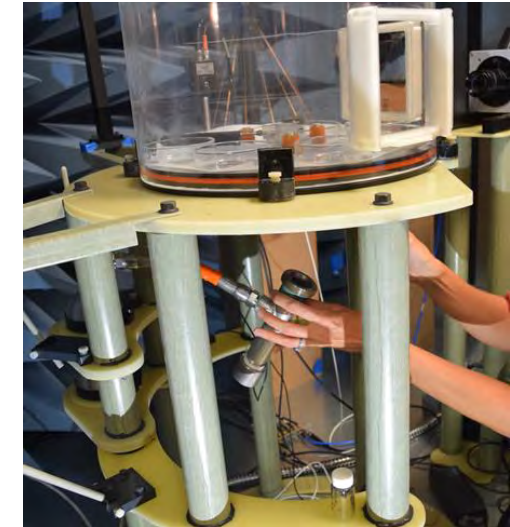
Photodiode



Discone to
0.125 GHz



Ice-captured CompB soot released from Al tube



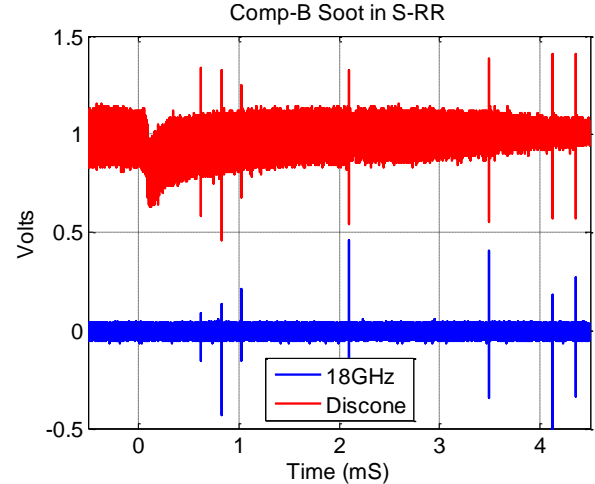
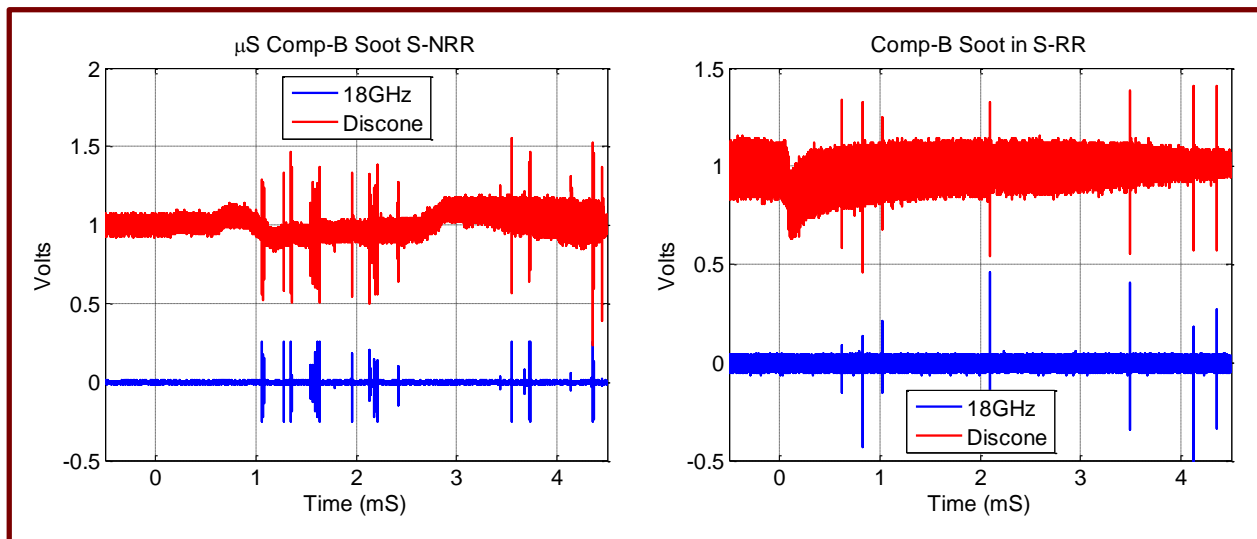
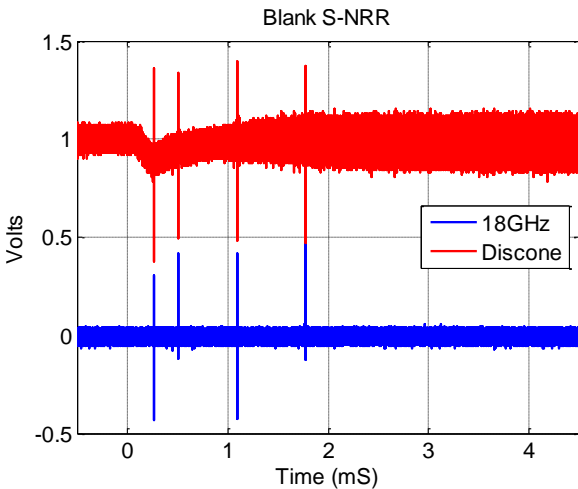
Sample loaded into base of shock tube where pressure is highest (~1000 psi).

No discharges observed above nozzle

Blank (LHS) vs. ice-captured CompB soot in Al tube (center), and CompB soot in nozzle (RHS)

Sample at base of Al shock tube

Sample in nozzle



More RF emissions with μ s Comp-B soot introduced from Al tube relative to blank and to Comp-B soot introduced from nozzle.

Summary of Results, Path Forward

- ▶ Revised STOA built and residing in dedicated anechoic chamber
- ▶ Insights into CDP charging provided by U of OR studies
- ▶ 9 shots on 9/9/21
 - Preliminary results: More RF emissions recorded with soot from base of shock tube relative to control, and relative to from nozzle, but diamond discharges observed with nozzle release.
 - New diagnostics include mm-wave antennas and will include particle charge measurements in support of charging simulations
 - New nozzles permit introduction of small particle quantities with reduced particle to Al wall charging
 - Better mixing of soot required? Higher pressures needed?
 - Signals equally large on Discone and Quad ridge antennas with ms CompB soot.
 - Further differentiation between frequency ranges not made yet.
 - 'Isolated' metal PT_n still providing discharge path. Will relocate.
 - ▶ YEAR 3: (a) continued STOA studies with improved diagnostics
 - (b) RF measurements with CDP vs. non-CDP producing HE, and
 - (c) measurement of mass and charge on CDP produced by HE detonations in the ms regime.

Impact

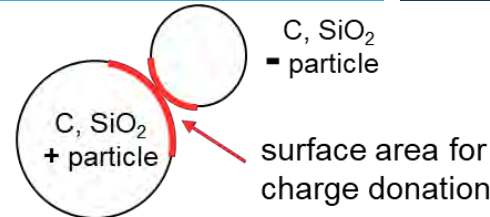
- Manuscript demonstrating consistency between experiment and hydrodynamic and electrostatic models submitted with LLNL, U of FL, LMU: "Standing shock prevents propagation of sparks in supersonic explosive flows," J. Von der Linden, C. Kimblin, I. McKenna, et al., scheduled for publication in *Communications Earth & Environment* on 20 Sept. 2021, <https://www.nature.com/commsenv/>, DOI: 10.1038/s43247-021-00263-y
- APS Conference: "Standing Shock Regulates Sparks in Explosive Flows," APS Division of Fluid Dynamics, Nov. 22, 2020, presented by J. Von der Linden
- APS Conference: "The Effect of Particles on Standing Shockwaves Regulating Spark Discharges in Volcanic Eruptions," 61st Annual Meeting of the APS Division of Plasma Physics, Oct. 24, 2019, presented by J. Von der Linden
- 2019 Fall AGU Meeting: "The Effect of Particles on Standing Shockwaves Regulating Spark Discharges in Volcanic Eruptions," Dec. 2019, poster presented by J. Von der Linden
- New collaborations
 - Professor Josef Dufek and Joshua Mendez-Harper (U. of OR)
- The SDRD-funded work allows us to participate in further DOE-funded work

Rapid Decompression Experiments

- ▶ Fluid dynamics in shock flow provides mechanism for charging, charge separation, and discharge
 - Particle charging by contact electrification, and separation by inertia.

1. Larger, like, particles thought to donate e's to smaller
2. Similarly sized particles separated into like-charged clusters by their relative Stokes numbers
3. Charge separation generates E-fields

- Rarefaction in shock flow may lower breakdown threshold, disrupting electron avalanche-to-streamer, to-leader hierarchy and influencing RF emission frequencies
- Behnke et al. JGR Atm, 2018: VHF RF; Mendez-Harper et al., GRL: 2018, barrel shaped discharge; this work with Sears, Kueny, von der Linden.



Kok, J. F. and N. O. Renno, *J. Geophys. Res.* **114** (2009).

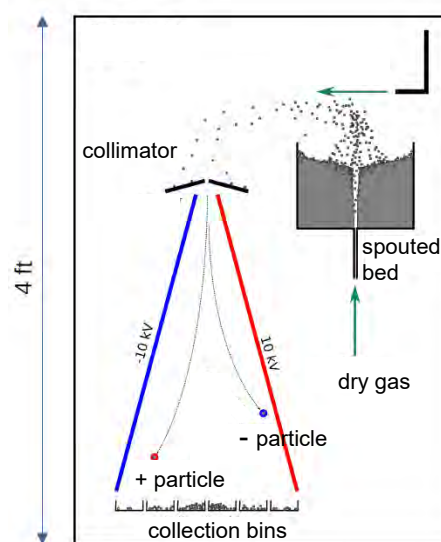
Species Composition at the CJ s

Species	TNT mol/kg	Comp B mol/kg	LX-10 mol/kg	NM mol/kg	AP-NM mol/kg	TRITONAL mol/kg	PETN mol/kg
—							
H2O	8.04	8.061	6.695		16.7	4.85	
CO2	7.491	7.045	6.813		6.702	1.146	
N2	6.286	10.29	12.63		5.301	4.773	
OH-	1.798	3.645	5.144		1.199	0.8374	
H+	1.798	3.645	6.511		4.076	0.8374	
CO	1.576	0.9256	1.906		0.0152	2.05	
NH3	0.632	0.7089	0.3924		0.000394	1.018	
CH4	6.69E-02	2.24E-02	1.11E-03		0	0.461	
H2	2.10E-02	6.92E-03	3.26E-04		0.000466	0.164	
C2H4	1.37E-02	3.39E-03	—		0	0.176	
C graphite	21.6	0	0	1.593	0	0.231	0
C diamond	0	12.7	7.162	0	0	0	0
C liquid	0	0	0	0	0	20.2	2.385
Al2O3	0	0	0	0	0	3.71	0

A. L. Kuhl, "Carbon Particles Produced by Detonation Waves," LLNL-CONF-703005, Sept. 2016

C particle charging behavior – U of OR

- ▶ Means to support shock tube studies and better understand C particle behavior
 - Fluidized bed studies to measure interparticle charging of diamond, graphite, and Comp B detonation soot
 - Measure charging rate, charge magnitude, and polarity at fluidization energies of 0.055–0.062 L/s in dry air
 - Detonation soot too aggregated for spouted bed

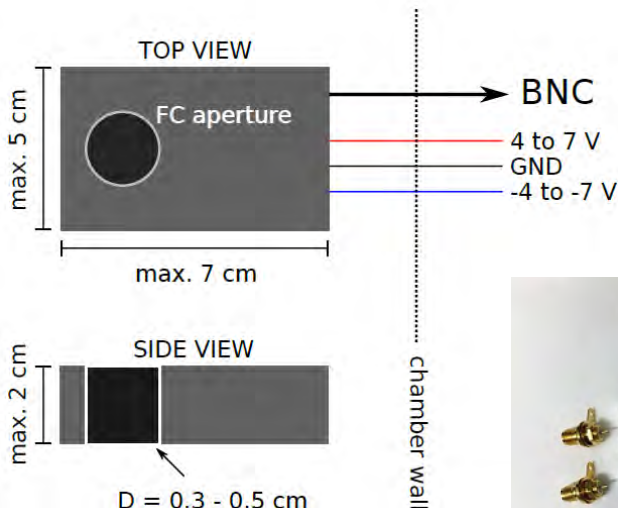


Large system required for **per particle** charge measurements with Faraday cup (FC) and electrostatic separator (ES)

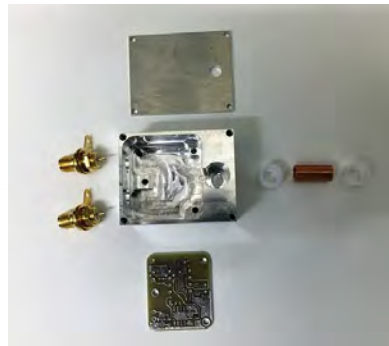


Through-type Faraday cup – U of OR

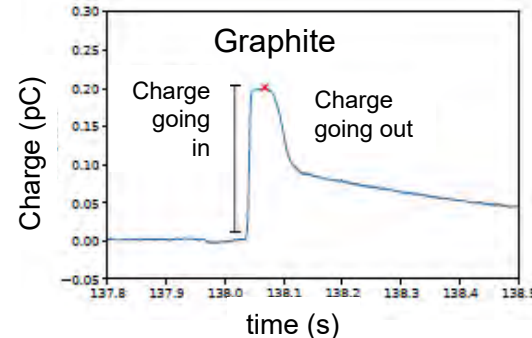
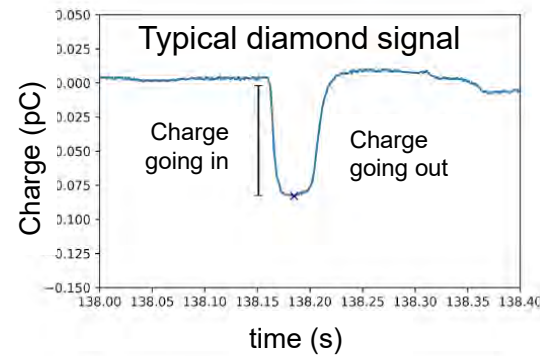
Faraday Cup – fully integrated version (single enclosure houses pre-amp and Faraday cup).



(drawings not to scale)



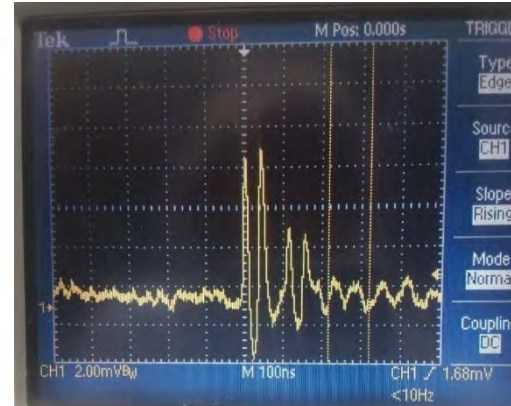
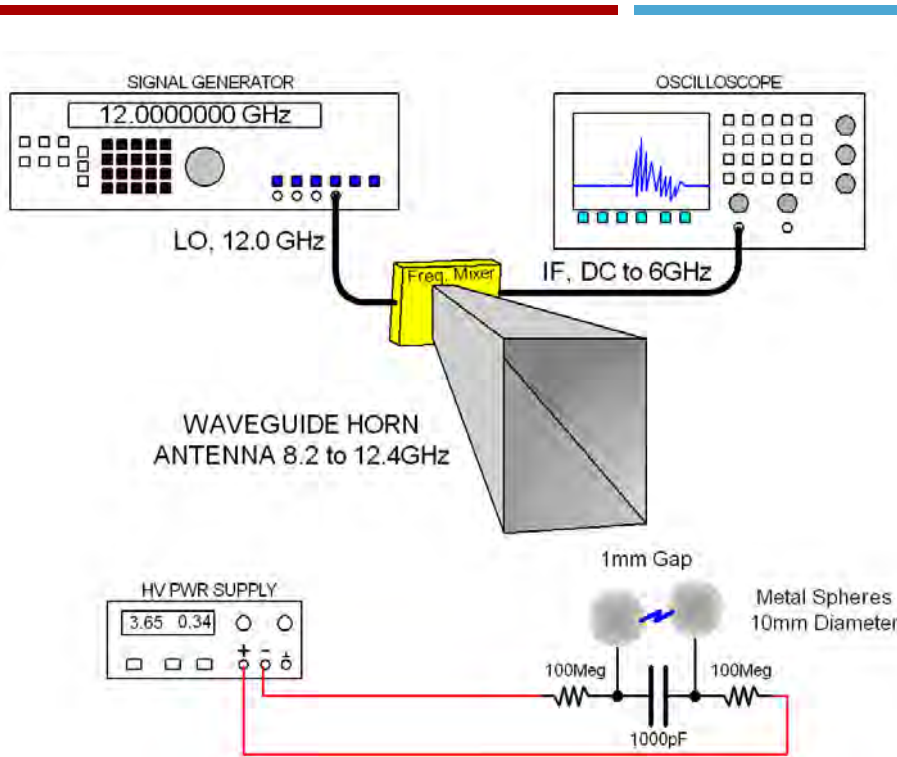
Aluminum enclosure, circuit board (without components), and sensing element



Graphite can display asymmetric signal in Faraday tube, loss of charge during collision.

12 GHz down-converter setup & output

23



12 GHz emission
associated with
1 mm spark
down- converted
to DC to 200 MHz.

1.9 micro-coulomb
charge transfer